AGU PUBLICATIONS

JGR

Journal of Geophysical Research: Atmospheres

RESEARCH ARTICLE
10.1002/2014JD022232

Key Points:
- Irrigation in California affects soil moisture and deep-layer percolation
- Effect of irrigation in California on precipitation is small
- ET in the Central Valley exhibits decrease trend

Correspondence to:
S. Sorooshian,
soroosh@uci.edu

Citation:
Sorooshian, S., A. AghaKouchak, and J. Li (2014), Influence of irrigation on land hydrological processes over California, *J. Geophys. Res. Atmos.*, *119*, 13,137–13,152, doi:10.1002/2014JD022232.

Received 26 JUN 2014
Accepted 31 OCT 2014
Accepted article online 10 NOV 2014
Published online 5 DEC 2014

Influence of irrigation on land hydrological processes over California

Soroosh Sorooshian[1], Amir AghaKouchak[1], and Jialun Li[1]

[1]Center for Hydrometeorology and Remote Sensing, Department of Civil and Environmental Engineering, University of California, Irvine, California, USA

Abstract In this study, a regional climate model (RCM) is employed to investigate the effect of irrigation on hydrology over California through implementing a "realistic irrigation" scheme. Our results indicate that the RCM with a realistic irrigation scheme commonly practiced in California can capture the soil moisture and evapotranspiration (ET) variation very well in comparison with the available in situ and remote sensing data. The RCM results show significant improvement in comparison with those outputs from the default run and the commonly used runs with fixed soil moisture at field capacity. Furthermore, the model reproduces the observed decreasing trends of the reference ET (i.e., ET0) from the California Irrigation Management Information System (CIMIS). The observed decreasing trend is most likely due to the decreasing trend of downward solar radiation shown by models and CIMIS observations. This issue is fundamental in projecting future irrigation water demand. The deep soil percolation rate changes depending on the irrigation method and irrigation duration. Finally, the model results show that precipitation change due to irrigation in California is relatively small in amount and mainly occurs along the midlatitudes in the western United States.

1. Introduction

Anthropogenic land cover and land use changes have dramatically altered the global land surface, especially with regard to the conversion of agriculture and pastures from natural lands [*Kueppers and Snyder*, 2012; *Ramankutty et al.*, 2008]. This conversion modifies the surface dynamical and thermodynamic features, such as roughness, albedo, and vegetation type and coverage, and affects the exchanges of water and energy between land surface and atmosphere and between land surface, soils, and aquifers. Agricultural practice processes, such as planting, fertilizing, irrigating, and harvesting, may also impact soil-land-atmospheric exchange processes in both biophysical and biogeochemical ways. Therefore, many numerical models, including global climate models (GCMs) and regional climate models (RCMs), have been employed to simulate these processes and the impacts of land conversions and land management practices on global/regional climate [e.g., *Avila et al.*, 2012; *de Noblet-Ducoudré et al.*, 2012] (also, see reviews of *Mahmood et al.* [2010] and *Pielke et al.* [2011]). However, few studies have been reported to investigate the impacts on hydrological processes using RCMs and/or GCMs, although irrigation may result in an increase in soil moisture, deep-layer percolation (or recharge), as well as the modification of surface runoff and river streamflow peaking, etc.

The impact of agricultural irrigation in California's Central Valley on the local/regional climate has been well reported based on numerical models, in situ observations, and remote sensing retrievals [*Adoegoke et al.*, 2003; *Bonfils and Duffy*, 2007; *Christy et al.*, 2006; *Kanamaru and Kanamitsu*, 2008; *Kueppers and Snyder*, 2012; *Kueppers et al.*, 2007, 2008; *Lobell and Bonfils*, 2008; *Lobell et al.*, 2009; *Ozdogan et al.*, 2010; *Sacks et al.*, 2009; *Sorooshian et al.*, 2011, 2012, and many others]. The results from models unanimously indicate that irrigation results in an increase in surface evapotranspiration (ET) and a decrease in low-level air temperature, although there are differences in amounts from different models. In order to mimic irrigation, the model root zone soil moisture in most of the numerical models is fixed at field capacity or even saturation in each integration time step. For example, *Kueppers and Snyder* [2012] investigated the surface flux (sensible, latent heat flux) variations from diurnal to seasonal scales through fixing the soil root zone moisture at field capacity at each time step. They argued that the surface ET and air temperature changes are very small when setting soil moisture to any values larger than 25% of the field capacity. *Lobell et al.* [2009] set the root zone soil moisture at saturation at each time step when they conducted the same study; they also concluded

that the irrigation-induced surface air temperature is insensitive to soil moisture when soil moisture is above 30% of saturation. At the very least, this model configuration [e.g., *Kueppers and Snyder*, 2012; *Lobell et al.*, 2009] results in improper description in soil hydrological processes, such as overestimating soil moisture variation and deep soil-layer percolation, which will be one of the items addressed in this manuscript.

Other investigators have made efforts to reasonably represent irrigation processes in the numerical models or to configure the proper amounts of water in the model root zone layers in order to improve model simulations. For example, *Kanamaru and Kanamitsu* [2008] found that setting up the root zone soil moisture at 50% of field capacity can reduce the model cool biases in a regional climate model (regional spectral model in their study). *Ozdogan et al.* [2010] conducted similar studies in an off-line land surface model (the Noah land surface model in their study), and their results (e.g., ET) are comparable with in situ observations. *Sorooshian et al.* [2011, 2012] implemented the recommended irrigation method suggested by *Hanson et al.* [2004], hereafter "realistic irrigation," into RCMs (MM5 and WRF). The RCM results (including ET, surface temperature, humidity, and wind) match well the in situ and remote sensing observations in different time scales (diurnal, annual, and interannual). However, irrigation-induced changes in the subsurface were not addressed.

It should be pointed out that similar to meteorologists' use of GCMs/RCMs to investigate the effects of irrigation on weather and climate, hydrologists have been using hydrological models to investigate the effects of agricultural irrigation on basin streamflow and water resources. For example, *Haddeland et al.* [2006] investigated the possible effect of irrigation in the Colorado River basin on streamflow, with the soil moisture in the VIC model set at fixed field capacity at each time step. *Pokhrel et al.* [2012] incorporated irrigation processes into a land surface model, in which a simplified TOPMODEL is coupled, to address water consumption and supply at the global scale. In their study, the horizontal resolution is 1°, which is relatively too coarse to represent the irrigation spatial features in the relatively narrow Central Valley and Imperial Valley of California. Additionally, the model soil moisture is fixed at 70% of field capacity at nonrice paddy irrigation regions without considering the differences of crop types to soil water stress. Specific to the Central Valley, 70% of field capacity still may be too high for most crops in comparison with field experiment results reported by *Hanson et al.* [2004]. *Hanson et al.* [2012] considered Central Valley irrigation water amounts based on water usage and supply in the commonly used groundwater flow model MODFLOW. The temporal and spatial scales used in their study were biweekly time scale and a ~0.2 km spatial resolution. In MODFLOW, the surface processes, including energy and mass processes, are treated in a relatively simple manner in comparison with grid point and physical-based land surface models (LSMs).

The investigation of irrigation-induced soil hydrology (i.e., water below the soil surface) is still necessary, both in understanding the physical processes such as water redistribution and variability, etc., and in examining physical model performances (see reviews of *Mahmood et al.* [2010] and *Pielke et al.* [2011]). In *Sorooshian et al.* [2011], an irrigation method is incorporated into the RCM, and the model performance was examined against available climate data with good results. In the second study [*Sorooshian et al.*, 2012], the effect of irrigation on ET was examined against remote sensing observations. In this third paper in the sequence, we focus on studying the effects of irrigation on land hydrological processes (e.g., surface runoff, groundwater recharge, and soil moisture) using RCM simulations, available observations, and off-line land surface model outputs from the North American Land Data Assimilation System (NLDAS) Phase 2.

2. Model Configuration and Data Collections

The mesoscale model National Center for Atmospheric Research (NCAR)/PENN STATE MM5, which has been used to study similar topics [e.g., *Segal et al.*, 1998; *Kueppers et al.*, 2008; *Sorooshian et al.*, 2011, 2012], is employed as the integration model. Since MM5 provides multiple choices of model physics schemes and model parameters, it is important to ensure that the selections are appropriate for the region of application. For this reason, we used sensitivity tests from the summer of 2007 to select the physics schemes and parameters for long-term runs at 18 km spatial resolution.

In the modeling system, the surface precipitation is derived using convective adjustment (i.e., the K-F convective parameterization scheme) and a grid-scale precipitation scheme [*Dudhia*, 1993]. Land hydrological processes are described using the Noah LSM [*Chen and Dudhia*, 2001; *Ek et al.*, 2003]. Soil moisture is resolved based on the Richardson equation that accounts for sources and sinks, such as precipitation and ET. Computation of

surface runoff is based on a simple water balance model, the excess precipitation not infiltrated into the subsurface [*Schaake et al.*, 1996]. The total evapotranspiration (ET) includes evaporation from the bare soil and canopy as well as transpiration from vegetation. The deep-layer percolation is defined as the Noah LSM [*Chen and Dudhia*, 2001].

For this study, three types of model runs are conducted to be forced by National Centers for Environmental Prediction reanalysis-I data. Run 1 is the "control" run (hereafter MM5C), which is the normal MM5 simulation run without any modifications. Run 2 is called the "field capacity" run (hereafter MM5F), where the MM5 root zone soil moisture is set to near-field capacity (i.e., 0.90% of field capacity in this study) at each time step. The conditions created for Run 2 are similar to those mentioned in some previous studies [e.g., *Haddeland et al.*, 2006; *Kueppers and Snyder*, 2012; *Kueppers et al.*, 2007, 2008; *Lobell et al.*, 2009]. Run 3 is called the "realistic" run (hereafter MM5R). For this case, and as was done in our previously reported studies, the soil moisture conditions are set up based on a number of factors, including the realistic irrigation of *Hanson et al.* [2004] and closely practiced by irrigators. In our MM5R run, irrigation water is applied when the following three conditions are satisfied: (1) the root zone's relative available soil water (SW) content is less than the maximum allowable soil water depletion (SW_m), where the magnitude of SW_m depends on the crop type and growth periods as discussed in *Hanson et al.* [2004], (2) when downward solar radiation is less than 50 Wm^{-2} for the purpose of model numerical stability during the simulations and for avoiding water loss due to ET at high solar radiation levels, and (3) soil temperature is greater than 10°C for the long-term run to avoid irrigating if the soil is frozen. Irrigation ceases when soil moisture reaches field capacity. In this paper, we mainly discuss variations of modeled hydrological variables, such as evapotranspiration (ET), soil moisture, surface and subsurface runoff, and percolation (recharge). The simulation studies are conducted at different time scales, and the results are compared with available observations and off-line land surface model outputs. The referenced data include the following:

1. NLDAS data. In brief, the NLDAS database provides model-generated hydrometeorological information from a number of available models (Noah, VIC, the Sacramento Soil Moisture Accounting, and Mosaic). For this study, ET, precipitation, gridded-surface runoff, soil moisture, and deep-layer percolation data generated from the Noah LSM in NLDAS version 2 [*Xia et al.*, 2012a] are used as reference data. The data are hourly and 0.125° horizontal resolution and are available since 1980 from the website (http://disc.sci.gsfc.nasa.gov/hydrology/data-holdings) (hereafter NLDAS). In NLDAS, precipitation is downscaled to hourly time step using daily, 0.25° spatial resolutions from the Climate Prediction Center (CPC) based on diurnal features of Stage II radar data. The other forcing data used in Noah-NLDAS are mostly downscaled from the North American Regional Reanalysis data set. The Noah LSM in the NLDAS version 2 has a few modifications to improve model performances [*Xia et al.*, 2012a; *Wei et al.*, 2012] as compared to previous versions. The changes include crop root estimates, leaf area index estimates, snow age and albedo estimates, vapor pressure deficit estimates in the canopy resistance, and the upper threshold of soil moisture at which the vegetation reacts to a soil moisture deficit, etc. For details, readers are referred to *Xia et al.* [2012a] and *Wei et al.* [2012]. In comparison with the Noah LSM that is coupled in MM5 and WRF, the Noah LSM in NLDAS version 1 is close to the Noah LSM in MM5, while the Noah LSM in NLDAS version 2 is close to the Noah LSM in WRF, which is used in this study.
2. MODIS ET. The MODIS ET data are downloaded from the Land Surface Hydrology Research Group at the University of Washington (http://ftp.hydro.washington.edu/pub/qiuhong/usa/) [*Tang et al.*, 2009]. The data are monthly at 0.05° spatial resolution and cover the whole U.S. from 2001 to 2008 (hereafter MODW). Another ET data set, generated by the Numerical Terradynamics Simulation Group at the University of Montana, is also based on MODIS data and is a 1 km sinusoidal projection which covers the years from 2000 to 2011 on a global basis (http://ntsg.umt.edu/project/mod16) [*Mu et al.*, 2011] (hereafter MODM).
3. Advanced Microwave Scanning Radiometer–EOS (AMSR-E) soil moisture. Surface soil moisture data generated from AMSR-E observations at daily and 0.25° are used in this study. The data set is provided by *Owe et al.* [2008]. The retrieved method for this data set uses a forward modeling optimization procedure to solve a radiative transfer equation for both soil moisture and vegetation optical depth [*Owe et al.*, 2008].
4. In situ data. In addition to gridded data, the following in situ observations are also used in this study: (a) ET, solar radiation, and precipitation from the California Irrigation Management Information System (CIMIS) sites over the Central Valley and Imperial Valley. The equipment for CIMIS sites are calibrated

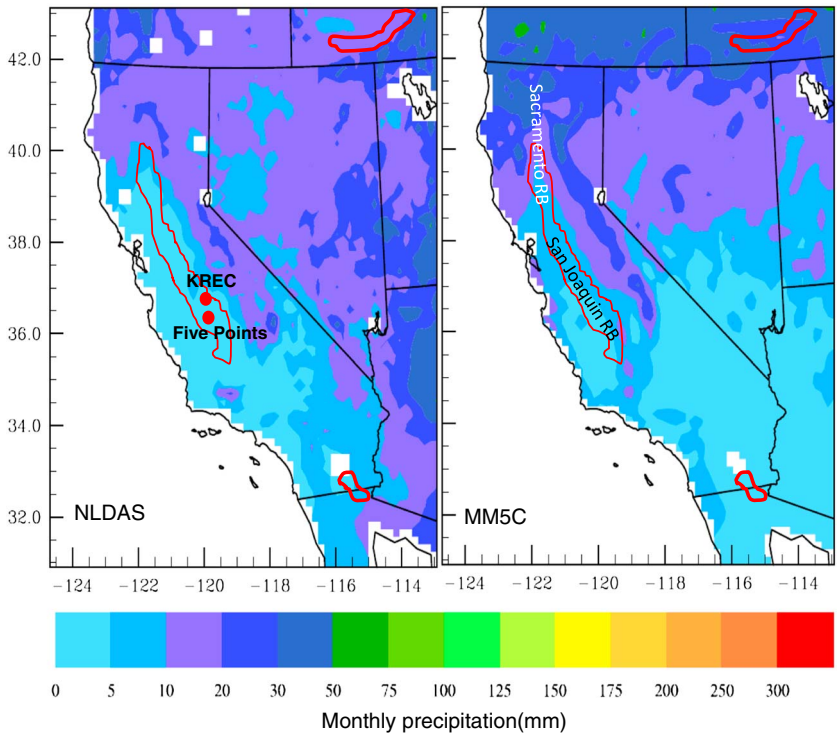

Figure 1. Monthly precipitation from MM5C and NLDAS-2 for June–September from 1981 to 2007. The red outlines indicate the locations of the irrigation areas. KREC and Five Points labeled in the left indicate the two in situ sites for ET and soil moisture.

annually, and data are quality-controlled at hourly, daily, and monthly time scales (B. Temesgen, personal communications, 2010) (also, see the CIMIS website). (b) Soil moisture data obtained from irrigated peach trees at the Kearney Research and Extension Center (KREC) at the University of California in Parlier and a cotton field at Five Points. The above in situ data sets have already been used in *Ozdogan et al.* [2010] and *Johnson et al.* [2002, 2004, 2005]. Therefore, the data quality should be reliable for this study. We should note that a few additional in situ measurement programs are also ongoing, but their data had not been released for public use at the time of this publication.

3. Results and Discussion

3.1. Precipitation

Precipitation is the key component in hydrological processes, and several studies have focused on changes in its trends and patterns [e.g., *Bell et al.*, 2004; *Duffy et al.*, 2006; *Gershunov et al.*, 2000; *Hao et al.*, 2013; *Leung and Qian*, 2009; *Damberg and AghaKouchak*, 2014]. Figure 1 shows the precipitation based on MM5C simulations and NLDAS forcing for June–September (i.e., the main irrigation months) from 1981 to 2007. As seen, summer precipitation is relatively small (primarily 0–20 mm/month), as confirmed by both data sets. However, in MM5C, precipitation is larger in midlatitude and mountainous regions than that in NLDAS forcing. Figure 1 also indicates that the model overestimates precipitation over most areas, except for the lee slope (eastward slope), where the model underestimates precipitation, and in the Tulare Basin in the southern Central Valley, where model precipitation and NLDAS precipitation are in good agreement.

Over the San Joaquin and Sacramento basins, precipitation is overestimated by 10–30 mm annually. However, in comparison with NLDAS precipitation, the MM5 overestimates by 50–80 mm annually, even more so in mountainous regions. NLDAS precipitation is originally based on 0.25° daily precipitation from the CPC. Some studies indicated that CPC precipitation data have dry biases, especially over the mountains [e.g., *Crow et al.*, 2009].

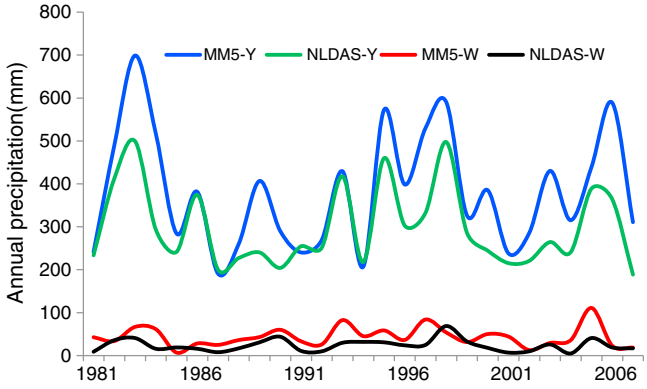

Figure 2. Mean precipitation time series over the irrigated grids in California: Annual total of MM5 (MM5-Y) and NLDAS (NLDAS-Y) and warm season accumulation of MM5 (MM5-W) and NLDAS (NLDAS-W). The warm season includes May–September. The precipitation is based on MM5C (control run).

Figure 2 shows the precipitation time series of annual totals in California irrigation areas (including the Imperial Valley) based on MM5 (line MM5-Y in Figure 2) and NLDAS (line NLDAS-Y in Figure 2). In this figure, precipitation is averaged over the irrigated region in California from MM5 (without an irrigation scheme). In comparison with NLDAS forcing precipitation, MM5 overestimates the annual precipitation by 30–50% (e.g., in 1983, 1984, 1989, 1995–1998, 2000, 2003, and 2006). Note that the precipitation variation of the two data sets indicates that the variability is mostly in phase with amplitude differences. Although some other hydrological variables, such as soil moisture and ET, are highly relevant to precipitation, our previous tests indicate that soil memory due to irrigation can last a maximum of about 1 month at the regional scale over the Central Valley [*Sorooshian et al.*, 2011]. This suggests that model precipitation biases in the cold season may not influence summer soil hydrological processes in the current model configuration. In Figure 2, MM5-W and NLDAS-W represent the accumulated annual precipitation time series averaged at irrigation grids over California from May to September. We note that the 5 month precipitation amounts are small ($<$60 mm for most of the years), averaging about 8.5 mm per month for MM5 and 4.8 mm per month for NLDAS forcing. The warm season precipitation feature also favors the analysis of modeled irrigation hydrological processes in the same seasons. In other words, because precipitation bias-induced soil moisture and ET variation can be minimized in the model system, we can address irrigation-induced hydrological processes with more confidence.

3.2. Evapotranspiration

Sorooshian et al. [2012] examined the ET variation from diurnal to interannual time scales and concluded that using a realistic irrigation method, model ET matches available remote sensing observations better than the control run, as well as the irrigation run when fixing the model root zone soil moisture at field capacity at each integration step. Here we extend the previous studies in the following aspects: (1) comparing model ET with the newly released NLDAS ET and in situ ET observations and (2) examining the ET long-term trend based on the model results and CIMIS reference ET.

Figure 3 displays the mean ET estimates of June–September 2001–2007 from different sources and shows the differences in amounts. In the figure, MODW indicates the remote sensing ET data generated by the hydrological research group at the University of Washington [*Tang et al.*, 2009]; MODM refers to the remote sensing ET data generated by the Numerical Terradynamics Simulation Group at the University of Montana [*Mu et al.*, 2011]. Although there are some differences in magnitudes, the ET spatial patterns are very consistent, indicating higher amounts along the coast and Sierra Nevada Mountains and lower amounts over the Great Basins and Death Valley. There are also high amounts along the irrigated agricultural areas over the Central Valley, the Imperial Valley, and the southern Idaho Valley. It should be noted that in MODM, ET over urban, water, and barren areas is masked.

The NLDAS ET shown in Figure 3 is based on the 2012 NLDAS version 2 Noah LSM [*Xia et al.*, 2012a, 2012b; *Wei et al.*, 2012]. This version includes crop root distribution, leaf area index seasonal variations, etc., which theoretically should improve ET estimates. However, the ET from the Noah LSM/NLDAS-2 still cannot capture the ET pattern over irrigation areas as observed by remote sensing data, especially in the Central Valley. On the other hand, RCM results with the realistic irrigation scheme can capture the spatial patterns similar to the ones captured by remote sensing data. Figure 3 also indicates that irrigation-induced ET varies in space and from one location to another, depending on soil features and weather conditions.

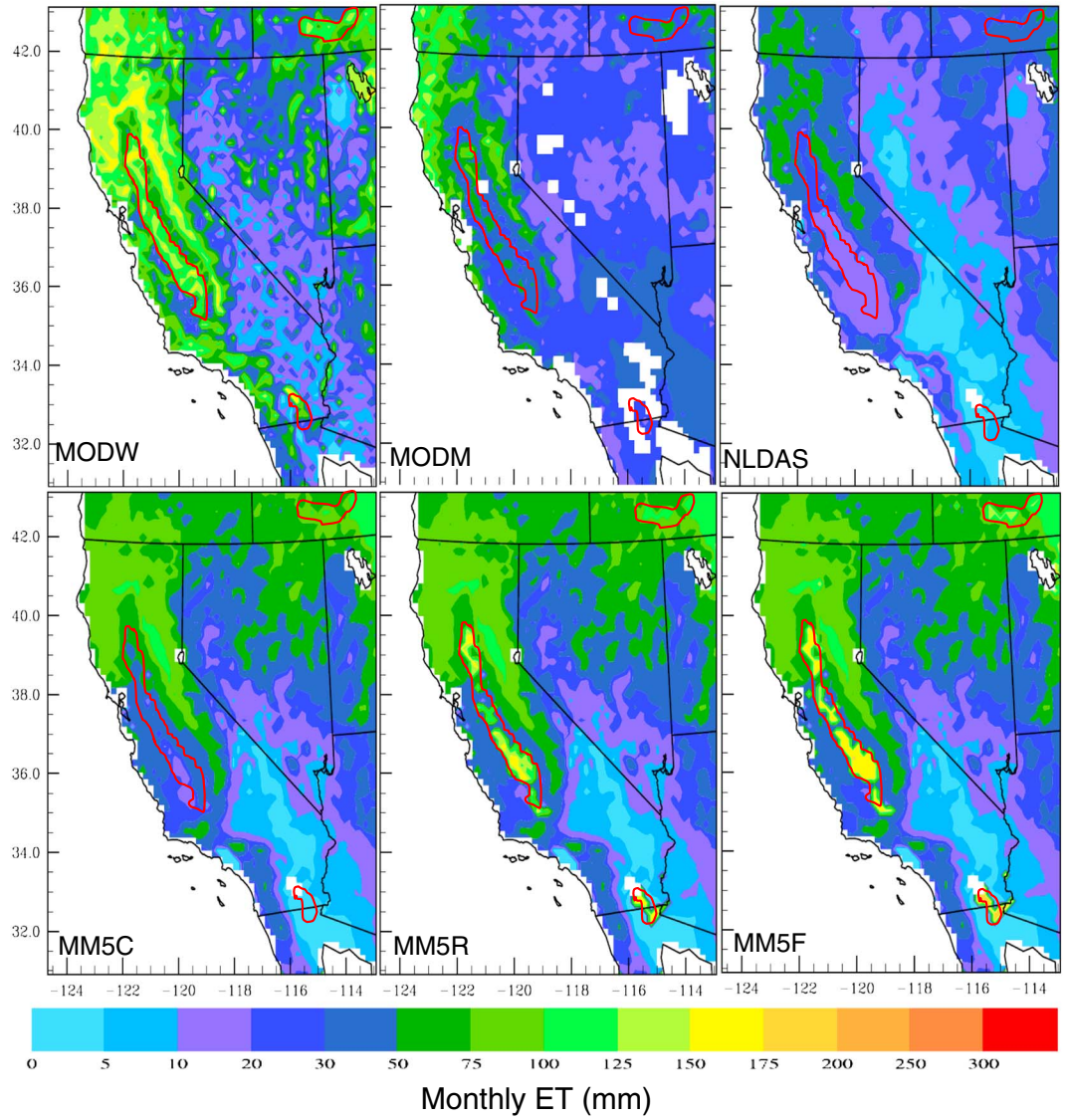

Figure 3. ET based on NLDAS (version 2 Noah LSM), MODW (MODIS-retrieved ET by the University of Washington), MODM (MODIS-retrieved ET by the University of Montana), MM5C, MM5R, and MM5F, averaged from June to September from 2001 to 2007. The red outlines indicate the approximate irrigation areas in southern Idaho, the Central Valley, and the Imperial Valley from top to bottom.

Figure 4 displays the ET comparison among in situ, model, and remote sensing at Five Points and the KREC in Parlier, California. In comparison with available in situ ET at the two sites (see Figure 1), RCM ET with the realistic irrigation scheme captures the peaks and the annual variation very well. MODIS ET (here MODW and MODM) and NLDAS-2/Noah, as well as MM5C, underestimate the ET relative to in situ observations. At Five Points, MM5R and MM5F are in very good agreement, while MM5F overestimates at the KREC site. Furthermore, both NLDAS Noah LSM outputs and MM5C ET indicate a phase shift because no water is added into soil, thereby resulting in drier soil during the dry seasons. It should be noted that the observed site at KREC was planted with peach trees starting in 1988, with the trees maturing in 1993. It is understandable that there is some difference between modeled ET and observed ET because the real water stress and water applications vary from year to year as the trees grow, while in the RCM irrigation mode the averaged monthly water stress of crops is used, which remains constant through the study years [*Sorooshian et al.*, 2011].

Figures 5a and 5b provide the multiyear time series of annual mean ET and monthly mean ET for July and August for 12 CIMIS sites in California and the model grid closest to the CIMIS site. The CIMIS sites are

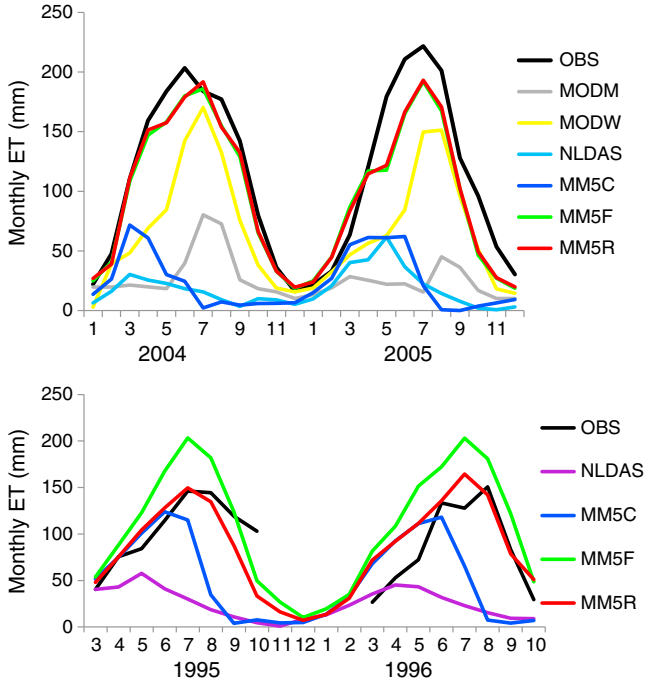

Figure 4. ET estimates based on in situ observations, remote sensing, and RCM and NLDAS grids closest to the observation site (a) at the Five Points cotton field and (b) at the peach trees close to the University of California Kearney Research and Extension Center (KREC) in Parlier, California. The locations of the sites are indicated in Figure 1.

selected if their records were longer than 20 years (i.e., before 1985). Figures 5a and 5b lead to the following conclusions:

1. CIMIS reference ET (ET0) over grassland when soil was saturated due to irrigation (see the CIMIS website) [see also *Sorooshian et al.*, 2011] shows interannual variations consistent with previous studies over irrigation regions [e.g., *Kueppers and Snyder*, 2012; *Kueppers et al.*, 2007; *Sorooshian et al.*, 2012].
2. The ET increases when the amount of irrigated water increases. ET0 is obtained when soil is saturated. In Figures 5a and 5b, MM5F ET is less than CIMIS ET0 because in MM5F, model root zone soil moisture is fixed to no less than 90% of field capacity, which is less than saturation conditions at each time step. We have examined ET variation at the CIMIS sites using the off-line Noah LSM and CIMIS meteorological fields as forcings. When fixing Noah LSM root zone layers at saturation, the Noah LSM ET matches CIMIS ET0 very well (not shown for brevity). This result is inconsistent with some of the previous studies, such as *Kueppers and Snyder* [2012] and *Lobell et al.* [2009], who concluded that when the amount of soil water is larger than 25% of field capacity or larger than 30% of saturation, the ET or near-surface air temperature is insensitive to soil water content. This difference between our results and the examples shown comes mainly from differences in the land surface parameterizations that are integrated into the climate model. Each LSM has its own parameterization scheme in estimating land-atmosphere water exchange coefficient, soil thermal and hydrologic conductivity, etc.
3. Both the model ET and CIMIS ET indicate a clear, long-term linear decreasing trend at annual mean as well as the average for July and August; furthermore, the more irrigation water that is applied, the more apparent the decreasing trend. However, both MM5C and NLDAS ET did not show these trends. As shown in Figure 2, both NLDAS precipitation and MM5 precipitation at the irrigation grid did not show any clear trends, either in annual mean or in the warm season accumulation. To identify a possible reason for this, we checked the model incoming radiation differences between irrigation runs and the control run. The results indicate that irrigation causes a decrease in downward long-wave radiation and appears to be statistically significant during the high-irrigation season (i.e., July and August) (see Figure 5d). Specifically, MM5R indicates an approximate 3.6 Wm^{-2} decrease in the downward long-wave radiation in comparison with MM5C, while MM5F shows a decrease of 5.51 Wm^{-2} relative to MM5C. A linear trend analysis indicates that MM5 model solar radiation decreased by about 3.7 Wm^{-2} per decade (Figure 5c), while downward long-wave radiation decreased by about 1.0 Wm^{-2} per decade (Figure 5d). We then evaluated the precipitation variation at the CIMIS sites, which is fairly close to the values of the nearest NLDAS grid cell. No long-term linear trends were detected (not shown for brevity). We also investigated the 2 m soil temperature, downward solar radiation, and humidity in some CIMIS sites. We noticed that the downward solar radiation shows a clear decreasing trend (about 4.0 Wm^{-2} per decade from 1984 to 2007), which is consistent with the model results.

The annual 2 m temperature and mixing ratio time series for July and August from MM5 is also exhibited in Figures 5e and 5f. In that figure, a decreasing trend for the 2 m temperature is shown, supporting the notion

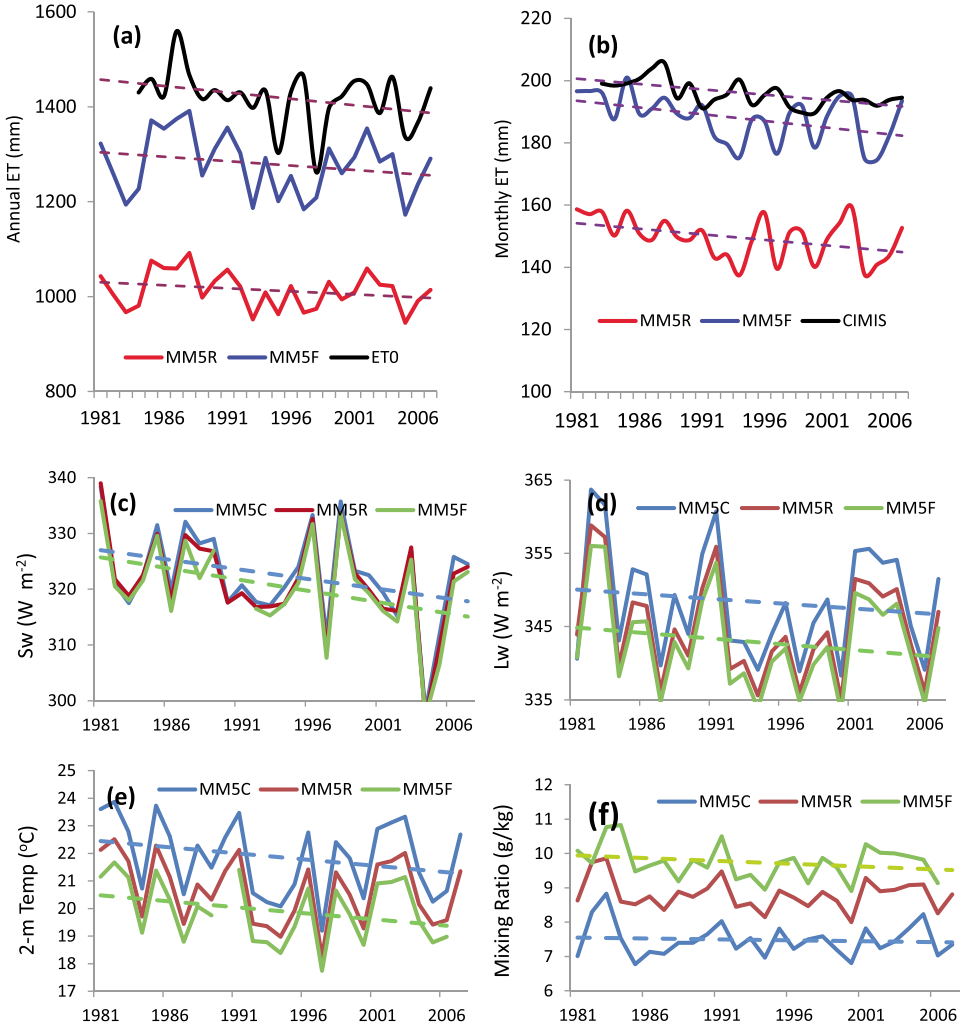

Figure 5. Mean irrigated grid variable time series over California from 1981 to 2007: (a) Annual total ET (mm), (b) mean ET from July and August, (c) downward solar radiation (Sw, Wm^{-2}) for July and August, (d) downward long-wave radiation (Lw: Wm^{-2}) for July and August, (e) 2 m air temperature (°C), and (f) 2 m mixing ratio (g/kg) for July and August. ET0 or CIMIS is the average from 12 CIMIS sites, where data records started before 1985.

that irrigation has resulted in a decrease in the 2 m air temperature. These results are consistent with some of the previous studies, such as *Bonfils and Lobell* [2007] and *Lobell and Bonfils* [2008].

Based on the above findings, we conclude that the irrigation-caused ET exhibits a decreasing trend, most likely due to decreasing solar radiation, downward long-wave radiation, and 2 m air temperature. Decreasing solar radiation and downward long-wave radiation may have caused a decrease in net radiation, which can impact the redistributions of net radiation between sensible and latent heat fluxes since the albedo and emissivity in the Noah LSM are irrigation independent.

Recently, *Pu and Dickinson* [2012] reported a similar phenomenon, namely, that ET has been experiencing a decreased trend due to vegetation feedback owing to increases in the greenhouse effect.

4. NLDAS ET is smaller than MM5C ET mainly due to the fact that MM5 overestimates precipitation, as indicated in the previous section. However, the variations of the two ET data sets are consistently in phase and out phase with the ET when irrigation is added at the interannual scale.

3.3. Soil Moisture

We first evaluated the remotely sensed soil moisture data and noticed that their quality is quite low, both in terms of resolution and missing data. Figure 6 displays an example of AMSR-E topsoil wetness mean for

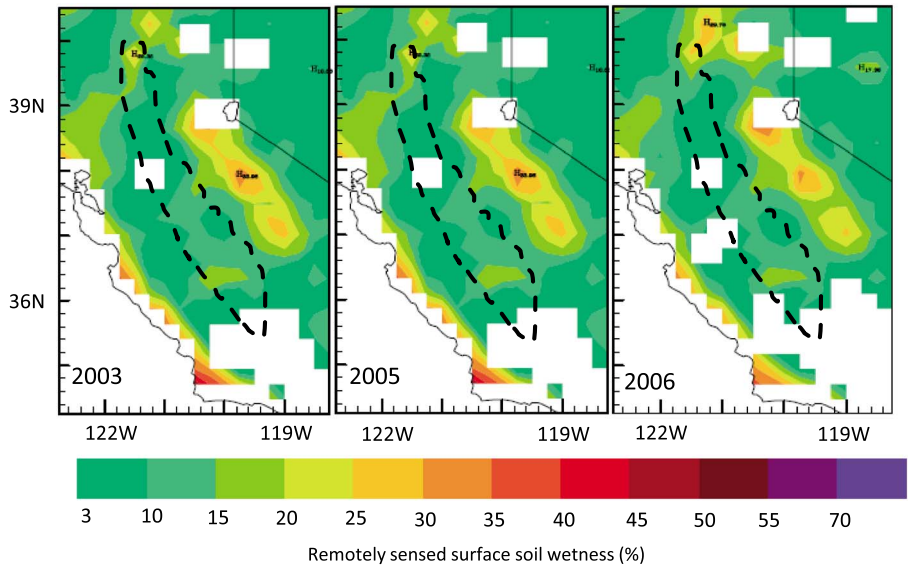

Figure 6. AMSR-E remotely sensed surface soil wetness (soil moisture to saturated soil moisture) averaged from July and August. Due to the coarse resolution (~40 km) of the remotely sensed data, it is difficult to recognize the effect of irrigation, except in the San Joaquin and Tulare basins, where the irrigation areas are large.

July and August for 2003, 2005, and 2006 based on the data of *Owe et al.* [2008]. Figure 6 also shows that the irrigation signature is reasonably captured where irrigation areas are large enough to be resolved in current AMSR-E 25 km resolution (e.g., over the southern San Joaquin Valley and the Tulare Basin). The soil wetness over the valleys displayed in Figure 6 is about 3%–20%. Based on the definition of soil wetness (i.e., the ratio of soil moisture to porosity), one can estimate that if soil is saturated, the wetness is 100%, and if soil moisture is at the field capacity level, the wetness should be about 60%–85%, depending on soil texture. The wetness over the Central Valley indicated in Figure 6 is far below the field capacity. Therefore, we can safely state that the model root zone soil moisture reaching 70% of field capacity overstates the irrigation impact on hydrological processes over the Central Valley. Over other areas where the irrigation areal extent is smaller than the AMSR-E (~25 km grid) resolution, AMSR-E cannot be used to identify the irrigation-induced soil wetness variation.

Currently, the availability of in situ soil moisture data is a limiting factor for validation and model-testing purposes. We obtained one site where the soil moisture was measured at an irrigated peach tree field (i.e., at the KREC in Parlier, California). Figure 7 displays the comparison between the observed and modeled grid soil moisture closest to the observation site. The top portion of the figure gives a comparison of the first model layer with different irrigation setups and the observations at depths of 1.5 in. (3.81 cm) and 2.5 in. (6.35 cm). The bottom section of the figure is similar to the top one, but at 4.5 in. (11.45 cm) and 5.5 in. (13.97 cm) for observations and the second model soil layer. The comparisons show that soil moisture from MM5R matches the observation fairly well but with a slight underestimation. In the case of the other two model configurations, MM5C highly underestimated and MM5F highly overestimated the observations. Despite its slight underestimation, MM5R clearly performed much better than the other two runs. Unfortunately, there were no in situ observations in deep soil layers for comparison. In general, and as clearly demonstrated in Figure 7, the model setup and the irrigation scheme can be used to examine the soil moisture variation over the irrigation areas in the Central Valley and even for all other irrigation areas in California

Figure 8 displays the model mean soil moisture interannual variation at the top and bottom soil layers in the irrigated grids (both Central and Imperial Valleys). In MM5, crop root is set to the first three layers with no consideration of seasonal and spatial differences. Thus, soil water is evaporated and/or transpired by the bare soil surface and any vegetation roots present in the top three layers. During the long and dry (no rainfall) seasons, the soil water will be eventually diminished to a wilting point through the vegetation root uptake

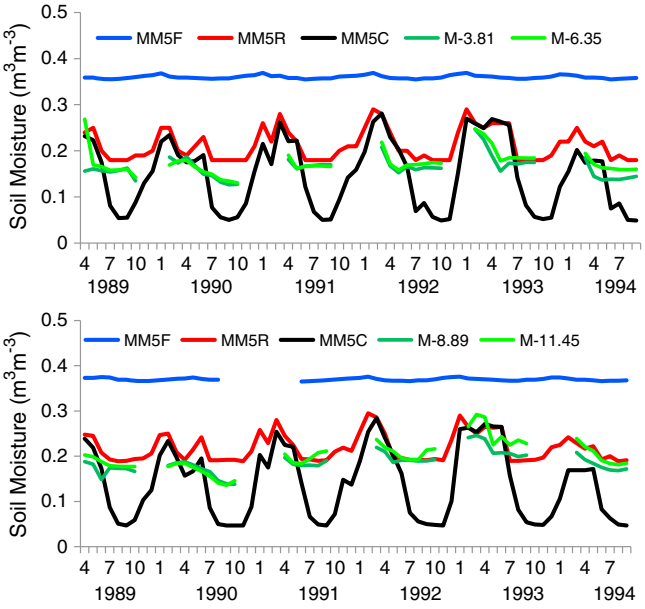

Figure 7. Model simulations and observations of soil moisture over the observation site: (a) first layer of the model and (b) second layer of the model (no field observations available from November to February).

and evapotranspiration. Hence, the model soil moisture at the top three layers has very similar variation, in contrast to the real world, due to the homogenous crop root distribution features in the MM5/Noah LSM. Figure 8 also shows that the amplitude of the soil moisture variation weakens more when more irrigation water is applied. The average soil water content at the top layer is about 17.5 mm (varying from 16 mm to 21 mm), 27.3 mm (varying from 26.5 mm to 28.5 mm), and 36.6 mm (varying about 0.2 mm), for MM5C, MM5R, and MM5F, respectively. In other words, irrigation decreases the seasonal and interannual variability of soil moisture in comparison with the control run.

Comparing the soil moisture of the MM5 control run with NLDAS, one can see that soil water content estimates from NLDAS/Noah LSM are slightly lower (−1.8 mm on average) than the MM5 control run (MM5C) in the top layer and much lower (−33.8 mm on average) in the bottom layer. This is because (1) MM5 generates more rainfall than NLDAS forcing during the same periods (see Figures 1 and 2) and (2) in NLDAS/Noah LSM, the upper threshold of soil moisture at which the vegetation reacts to a soil moisture deficit has been adjusted [*Xia et al.*, 2012a; *Wei et al.*, 2012], compared to the Noah LSM in MM5. However, soil water contents from MM5C and NLDAS/Noah have the same interannual variations. Figure 8 indicates that MM5C has basically reproduced the soil water content variations as shown in the NLDAS-2 Noah LSM output with observation/analysis forcings, demonstrating that our model outputs are reliable.

3.4. Surface Runoff

In this study, we focus mainly on grid cell hydrology at irrigation areas in California. It should be noted that water in California is highly regulated by dams and multilevel (local, state, and federal) water transportation projects across the state, which makes it difficult to simulate the horizontal flow of water at basin scale. From June to September (JJAS) each year, rainfall precipitates primarily over the Serra Nevada Mountains and the elevated Northern California regions, with very limited rainfall over the irrigation areas (see outputs of

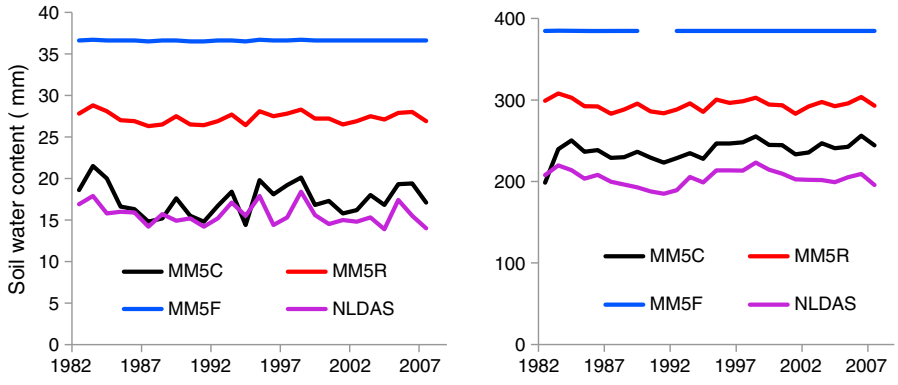

Figure 8. Irrigation grid-averaged soil water content (mm) interannual variation at (left) top layer and (right) bottom layer. The raw MM5F output from June 1990 to May 1991 was missing.

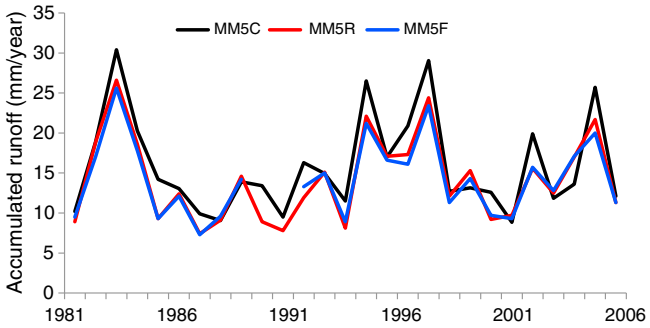

Figure 9. Annual accumulated surface grid runoff over irrigation areas in California. The raw MM5F output from June 1990 to May 1991 was missing.

MM5C, MM5R, MM5F, and NLDAS presented in Figures 1–3). Therefore, surface runoff occurs mainly over the mountains and the higher-elevation areas in Northern California. In JJAS, and based on MM5C, MM5R, MM5F, and NLDAS/Noah outputs, the surface-gridded runoff over the irrigation areas (Central Valley and Imperial Valley) is less than 1 mm per month (not shown). Figure 9 exhibits the accumulated "gridded" surface runoff for MM5C/R/F over irrigation areas in California during the water year. In comparison with amounts of ET and precipitation presented earlier, surface runoff is a relatively small component of the water cycle during the summer, especially in the irrigation season (JJAS).

3.5. Deep-Layer Percolation and Water Balance

In the following section, we discuss the deep-layer percolation component of the soil hydrology over the study area. The amounts of the deep-layer percolation are the outputs of MM5-coupled land-vegetation (crop) atmospheric model, the NLDAS off-line simulations, and the results from previously published studies. In the control and irrigation runs, grid cell soil moisture variation at a specific time interval ideally can be written as follows:

$$\frac{dm_c}{dt} = P_c - E_c - R_c - D_c \tag{1}$$

$$\frac{dm_i}{dt} = P_i + I_i - E_i - R_i - D_i \tag{2}$$

where m is soil water content, P is precipitation, I is irrigated water, E is ET, R is surface runoff, and D is deep-layer recharge during the time period. In equations (1) and (2), the subscripts c and i represent control run and irrigation run, respectively.

From Figures 1, 2, and 11, one can conclude that the irrigation-induced precipitation and surface runoff are relatively small components of the water cycle (see Figure 10). The long-term soil moisture changes are not significant in arid/semiarid areas because the soil moisture depletes rapidly through evaporation and reaches the wilting point in nonirrigation areas, while the water from the irrigation areas is continuously added to keep the soil water content at a certain level. Therefore, the total irrigation water can be approximated based on the differences of ET and recharge in the irrigation and control runs.

Table 1 shows the annual average water distribution over the irrigation grids in California between MM5C/R/F and NLDAS from 1981 to 2007. Table 2 is similar to Table 1, except that the distributions shown are for the San Joaquin and Tulare watersheds in June–September each year when precipitation is very little and heavy irrigation water is applied. Based on equation (1) and the data given in Tables 1 and 2, the total irrigation water and irrigation-induced deep-layer percolation rate can be estimated. At the annual scale over California, the estimate for irrigation water based on the MM5R run is about 758 mm yr^{-1}, while the MM5F run gives a value of 1230 mm yr^{-1}. At the peak of the season, the irrigation water over the southern part of the Central Valley is estimated by the MM5R run to be about 126.6 mm per month and about 160.4 mm per month based on the MM5F run. The percolation rate due to irrigation is estimated to be approximately 5% based on MM5R and 17.6% based on MM5F over the southern part of the Central Valley in the summer time. Over the entire California irrigation areas, the annual percolation rate is about 18% based on MM5R and 28% based on MM5F, respectively. These estimates indicate that with a realistic irrigation scheme incorporated into MM5R, the percolation rate due to irrigation is substantially less than the commonly used irrigation at field capacity assumed in MM5F. The obvious question is which is closer to in situ and more trusted values.

Unfortunately, consistent and long-term field observations of the percolation rates are not available. However, the closest we can get to in situ observations are those estimates provided by *Wichelns and Nelson* [1989].

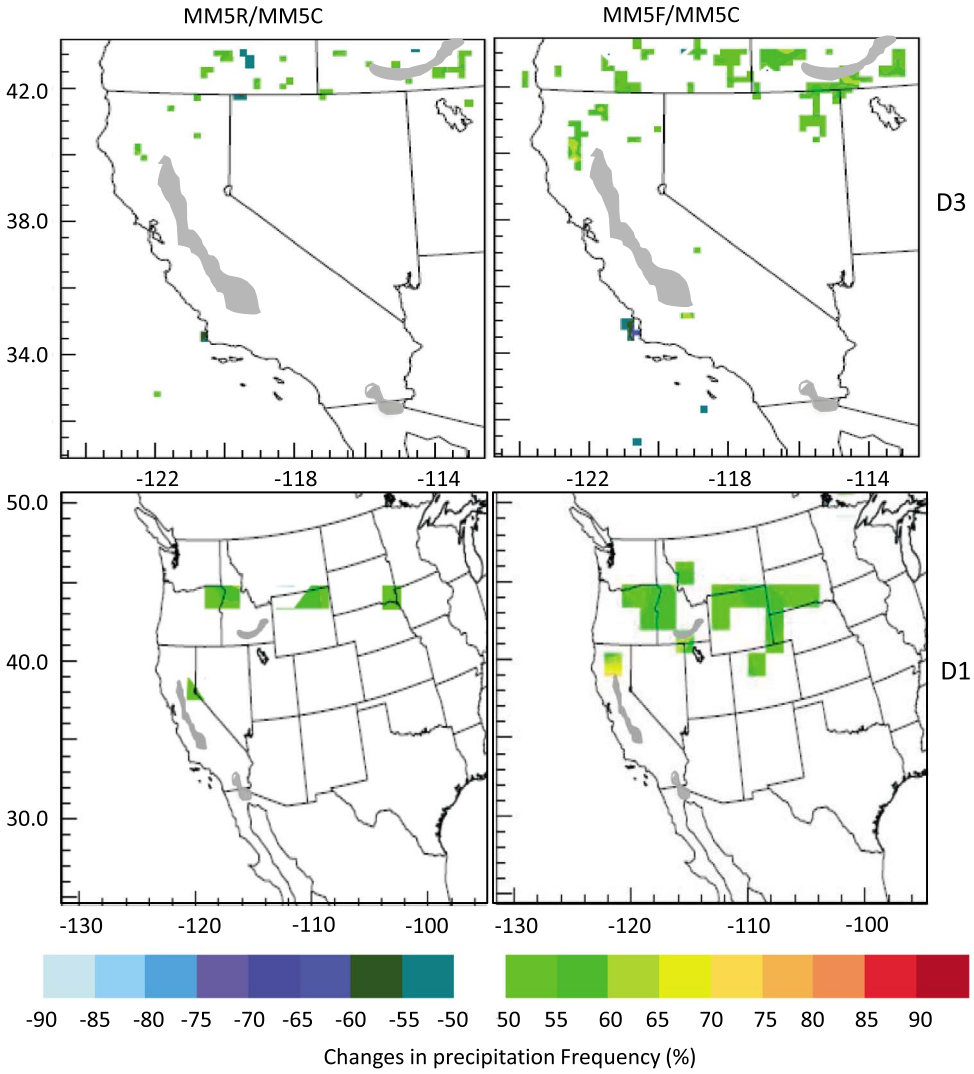

Figure 10. Changes in precipitation frequency (%) due to irrigation in comparison with the control run. Monthly rainfall with irrigation is greater/less than 0.3 mm per month to that without irrigation is counted. The grey-filled areas are irrigation locations: (top) 162 km resolution and (bottom) 18 km resolution.

They estimated deep soil-layer percolation rates at different locations in the San Joaquin Basin with 23% in 1986, 20% in 1987, and 18% in 1988. These values are very close to the model results from MM5R. The California State Water Resources Control Board (1992) reported the relationship of the irrigated water and deep drainage. The average percolation rates of 1989 and 1990 are 14% for subsurface drip irrigation (similar to our MM5R setup), 26% for low-energy precision application, and 30%–64% for furrow irrigation, which means that the percolation rate depends highly on the irrigation methods as well. Nevertheless, based on these limited reported observation estimates, we feel comfortable in suggesting that the MM5R-generated percolation rate is close to the field measurement for most of the experiments.

Table 1. Annual Average Water Distribution Over the Irrigation Regions in California

	Precipitation (mm)	ET (mm)	Surface Runoff (mm)	Recharge (mm)	Soil Water Changes (mm)
MM5C	448.1	385.8	15.9	98.4	1.2
MM5R	450.1	1000.9	13.9	241.1	−0.5
MM5F	453.0	1268.7	14.0	452.0	0.0
NLDAS	290.7	254.5	10.6	39.0	−1.9

Table 2. June–September Water Distribution Over the Irrigation Regions in the San Joaquin and Tulare Watersheds

	Precipitation (mm per month)	ET (mm per month)	Surface Runoff (mm per month)	Recharge (mm per month)	Soil Water Change (mm per month)
MM5C	6.7	29.2	0.1	1.3	−21.6
MM5R	7.1	130.8	0.0	7.6	−8.9
MM5F	7.9	159.8	0.0	29.5	0
NLDAS	2.1	14.4	0.0	0.2	−9.6

3.6. Where and How Far Does the Evapotranspired Water Travel From the Central Valley Irrigation Region?

In our 2011 work [*Sorooshian et al.*, 2011], we analyzed the changes in meteorological variables at the locations more than 10 km in distances from irrigation areas relative to observations. Our results showed that the absolute differences between irrigation and nonirrigation runs were much smaller than those between irrigation/nonirrigation and observations. We concluded that irrigation-induced climatic change in Central Valley, California, is very small at the nonirrigation areas a few tens of kilometers away from the irrigation regions.

In this study, we analyze the effect of irrigation on precipitation in warm seasons (June–September) for the period of 1981–2007 in California and Southern Idaho. Figure 10 shows the changes in precipitation frequencies at different model resolutions due to irrigation (irrigation areas are marked with gray). In Figure 10, the monthly accumulated precipitation differences between the irrigation and control runs (−0.3 to 0.3 mm) is masked. The results show that while adding more water in the irrigation areas may generate slightly more precipitation outside the irrigation region, precipitation occurs mainly in midlatitude regions, such as Oregon, Idaho, Wyoming, and South Dakota, with no significant rainfall differences detectable in the southwestern United States. We have also used precipitation differences at 3 mm per month as a threshold to examine the effects of irrigation on precipitation and found no rainfall differences between the irrigation runs and the control run. In other words, our model-based results show that increases in irrigation-induced precipitation could be in the range of 0.01–0.1 mm d^{-1}, which indicates that the precipitation change due to irrigation is less than 1% during the warm season.

Recently, there have been a number of reported studies presenting model simulation results regarding the fate and the extent of the influence of ET water from California's Central Valley irrigation region. Using version 3.5 of the NCAR Community Atmosphere Model, combined with version 3.5 of the Community Land Model and prescribing irrigation water based on the work of *Wisser et al*. [2008] in the Central Valley irrigation areas at the resolution of T85 (approximately 1.4° × 1.4°), *Lo and Famiglietti* [2013] reported that precipitation in the southwestern U.S. increases by 15% in the summer (June–August) and streamflow in the Colorado River increases by about 30% because of Central Valley irrigation. In another study, *Wei et al.* [2013] used the Modern-Era Retrospective Analysis for Research and Applications system and the quasi-isentropic back-trajectory method [*Dirmeyer and Brubaker*, 1999, 2007] to trace the water vapor for each precipitation event backward in time. The tracing was done along the isentropic surface starting from the grid box with precipitation backward in space and time until all of the original precipitation is attributed to ET. They found that California irrigation-induced precipitation occurs mainly from the Sierra Nevada Mountains eastward along the midlatitude and with less than 1% of total precipitation in most of the areas (see their Figures 6 and 10). Our results, which are close to those of *Wei et al.* [2013], are different (in both spatial distribution and amount) than those recently reported by *Lo and Famiglietti* [2013]. The differences could be due to a number of factors, such as model resolution, model physics, parameterization, land use/land cover representation, and boundary conditions. Figure 11 presents the total column water vapor flux average from the control run in JJAS. This circulation pattern favors the scenario that the evaporated water (from irrigation regions) was transported eastward and into midlatitudes due to wind patterns.

3.7. Transferability of the Proposed Irrigation Scheme

Based on the comments from reviewers, we have implemented the same irrigation scheme into the Weather Research and Forecast (WRF) model (version 3.3.1), and the results are similar. As an example, Figure 12 shows the simulated average 2 m temperature changes due to the irrigation at different times for June–August

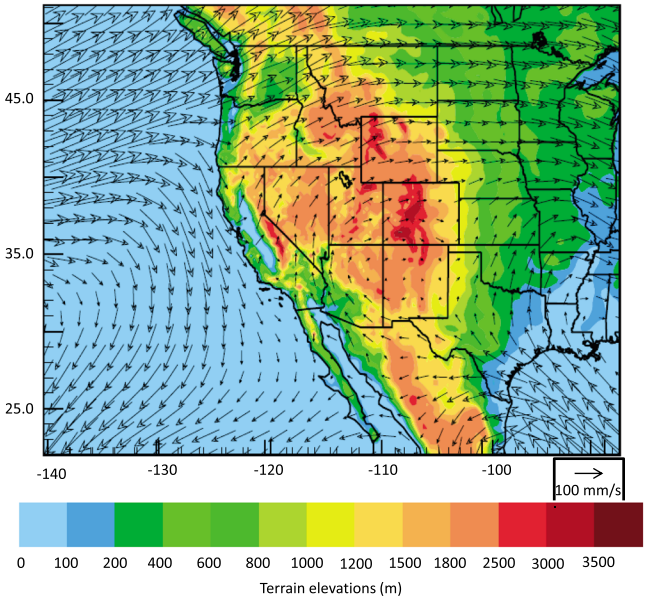

Figure 11. Modeled water vapor fluxes (entire vertical column) for the control run.

in 2007. It is evident from the depicted simulation results that the MM5 and WRF reproduce similar temperature differences with and without the irrigation scheme (i.e., MM5R-MM5C and WRFR-WRFC).

4. Conclusions

The impacts of agricultural irrigation on hydrological processes over California have been investigated using the regional climate model (RCM), an off-line land surface model output, and available in situ observation and remote sensing data. Our results indicate that by implementing a realistic irrigation scheme, one can reasonably capture the irrigation-induced ET, soil moisture, and percolation variations and reproduce observed patterns and previous field reports [e.g., *Wichelns and*

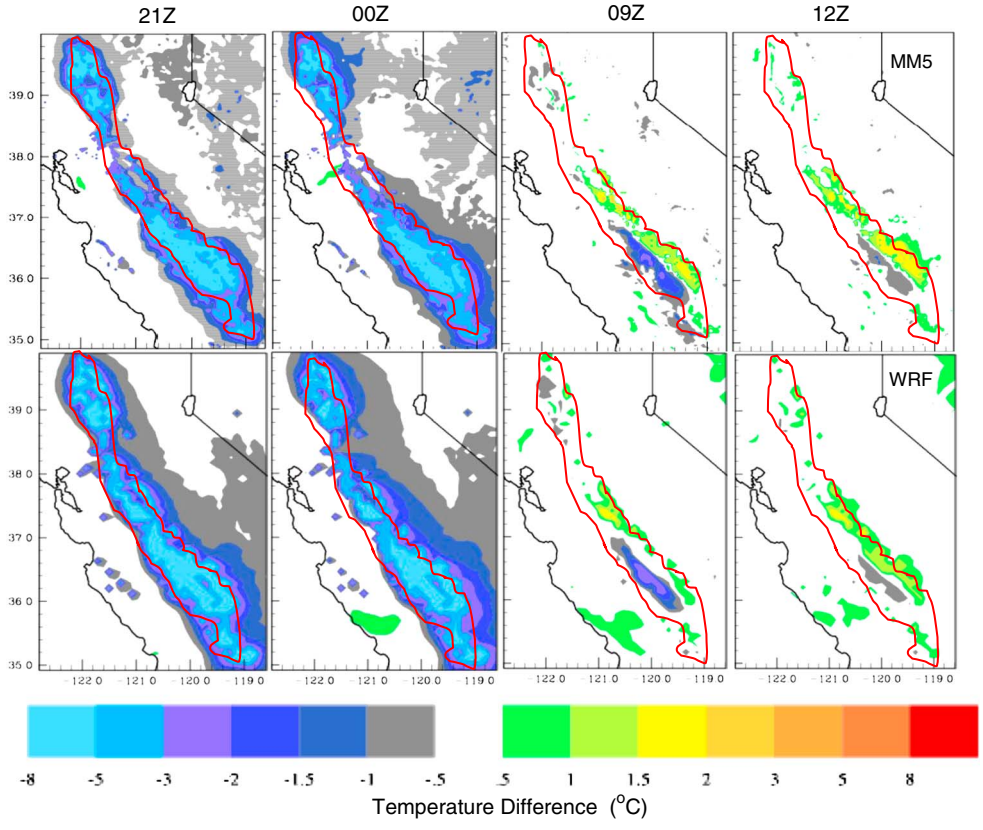

Figure 12. MM5 and WRF simulations of temperature differences with and without the irrigation scheme used in this study (i.e., MM5R-MM5C and WRFR-WRFC). The figure shows the averages of June–August 2007.

Nelson, 1989]. Without consideration of the irrigation processes in physically based models, neither the MM5 control run nor the improved Noah LSM off-line run (e.g., NLDAS) can capture the irrigation-induced hydrological patterns. On the other extreme, to fix the model root zone soil moisture as field capacity or saturated at each time step, the model overestimates evapotranspiration and deep-layer percolation, which is inconsistent with available field measurement reports and remote sensing observations. The realistic irrigation method adapted in our study can be used to more accurately estimate the influence of irrigation water applications over California, either in the hydrological model or in the water resources management model.

Model results also indicate that irrigation-induced ET exhibits long-term linear decreasing trends. The RCM ET long-term linear trend is consistent with the variation of the CIMIS reference ET, which is estimated from the in situ field measurements. The reason for this decreasing trend is the observed downward short-wave radiation trend, which consequently impacts the net radiation and its redistributions between sensible heat fluxes and latent heat fluxes. The results show that the irrigation-induced precipitation variation outside of the irrigation area is very small (0.01–0.1 mm d^{-1}) and occurs mainly along the midlatitude areas. Our estimated values are consistent with reported magnitudes from more realistic observation-based studies [*Dirmeyer and Brubaker*, 1999, 2007; *Wei et al.*, 2013]. Our results also show significant inconsistency with the recently reported model simulation studies of *Lo and Famiglietti* [2013] in both spatial distribution and amount.

Although a model with a realistic irrigation scheme can basically capture the hydrological features observed, the model deficiencies are also apparent. Despite significant progress in the past decades, regional model simulations of precipitation have substantial biases that could affect irrigation water demand. For example, a wet bias in precipitation leads to less irrigation water demand than what is actually needed and vice versa.

In order to fully and realistically estimate the amounts of ET, soil moisture, and deep-layer percolation, the resolution of the modeling application must be at the field scale where the variations in crop types and their respective water stress differences can be captured. At the same time, more ground-based observations are needed for model validation and verification purposes. This will greatly improve model performance evaluations and allow for more effective ways of improving understanding of land hydrological processes in irrigated agricultural regions.

Acknowledgments

The authors thank James Ayars of the USAD ARS for providing the ground-based ET data at Five Points. The authors also thank Scott Johnson, University of California Kearney Research and Extension Center, for providing the in situ ET and soil moisture data at Parlier, California. This study is supported by the NOAA MAPP program (NA10OAR4310162) and the United States Bureau of Reclamation program (award R11AP81451). Interested readers can request the data from the authors (jialunl@uci.edu) or download the data from the following link: ftp://earth.eng.uci.edu/jialun/data/long-term/.

References

Adoegoke, J., R. Pielke Sr., J. Eastman, R. Mahmood, and K. Hubbard (2003), Impact of irrigation on midsummer surface fluxes and temperature under dry synoptic conditions: A regional atmospheric model study of the U.S. High Plains, *Mon. Weather Rev.*, *131*, 556–564.

Avila, F., A. Pitman, M. Donat, L. Alexander, and G. Abranmowitz (2012), Climate model simulated changes in temperature extremes due to land cover change, *J. Geophys. Res.*, *117*, D04108, doi:10.1029/2011JD016382.

Bell, J., L. Sloan, and M. Snyder (2004), Regional changes in extreme climatic events: A future climate scenario, *J. Clim.*, *17*, 81–87.

Bonfils, C., and P. Duffy (2007), Comments on "Methodology and results of calculating central California surface temperature trends: Evidence of human-induced climate change?", *J. Clim.*, *20*, 4486–4489.

Bonfils, C., and D. Lobell (2007), Empirical evidence for a recent slowdown in irrigation-induced cooling, *Proc. Natl. Acad. Sci. U.S.A.*, *104*, 13,582–13,587, doi:10.1073/pnas.0700144104.

Chen, F., and J. Dudhia (2001), Coupling an advanced land surface-hydrology model with the Penn State-NCAR MM5 modeling system, Part I: Model implementation and sensitivity, *Mon. Weather Rev.*, *129*, 569–585.

Christy, J. R., W. B. Norris, K. Redmond, and K. P. Gallo (2006), Methodology and results of calculating central California surface temperature trends: Evidence of human-induced climate change?, *J. Clim.*, *19*, 548–563.

Crow, W., G. Huffman, R. Bindlish, and T. Jackson (2009), Improving satellite-based rainfall accumulation estimates using spaceborne surface soil moisture retrievals, *J. Hydrometeorol.*, *10*, 199–212.

Damberg, L., and A. AghaKouchak (2014), Global trends and patterns of droughts from space, *Theor. Appl. Climatol.*, *117*(3), 441–448, doi:10.1007/s00704-013-1019-5.

de Noblet-Ducoudré, N., et al. (2012), Determining robust impacts of land-use induced land-cover changes on surface climate over North America and Eurasia: Results from the first set of LUCID experiments, *J. Clim.*, *25*, 3261–3281.

Dirmeyer, P., and K. Brubaker (1999), Contrasting evaporative moisture sources during the drought of 1988 and the flood of 1993, *J. Geophys. Res.*, *104*, 18,383–18,397, doi:10.1029/1999JC900119.

Dirmeyer, P., and K. Brubaker (2007), Characterization of the global hydrological cycle from a back-trajectory analysis of atmospheric water vapor, *J. Hydrometeorol.*, *8*, 20–37.

Dudhia, J. (1993), A non-hydrostatic version of the Pennn State-NCAR Mesoscale model: Validation Tests and simulation of an Atlantic Cycle and Cold front, *Mon. Weather Rev.*, *121*,1491–1513.

Duffy, P., et al. (2006), Simulations of present and future climates in the Western United States with four nested regional climate models, *J. Clim.*, *19*, 873–895.

Ek, M. B., K. E. Mitchell, Y. Lin, E. Rodgers, P. Grunman, V. Koren, G. Gayno, and J. D. Tarpley (2003), Implementation of Noah land surface model advances in the National Centers for Environmental Prediction operational mesoscale Eta model, *J. Geophys. Res.*, *108*(D22), 8851, doi:10.1029/2002JD003296.

Gershunov, A., T. Barnett, D. Cayan, T. Tubbs, and L. Goddard (2000), Prediction and downscaling ENSO impacts on intraseasonal prediction statistics in California: The 1997/98 event, *J. Hydrometeorol.*, *1*, 201–210.

Haddeland, I., D. Lettenmaier, and T. Skaugen (2006), Effects of irrigation on water and energy balances of the Colorado and Mekong river basins, *J. Hydrol.*, *324*, 210–223.

Hanson, B., L. Schwankl, and A. Fulton (2004), *Scheduling Irrigations: When and How Much Water to Apply?*, *Division of Agriculture and Natural Resources. Pub.*, vol. 3396, 202 pp., Univ. of California, Davis.

Hanson, R. T., L. E. Flint, A. L. Flint, M. D. Dettinger, C. C. Faunt, D. Cayan, and W. Schmid (2012), A method for physically based model analysis of conjunctive use in response to potential climate changes, *Water Resour. Res.*, *48*, W00L08, doi:10.1029/2011WR010774.

Hao, Z., A. AghaKouchak, and T. J. Phillips (2013), Changes in concurrent monthly precipitation and temperature extremes, *Environ. Res. Lett.*, *8*(4), 034014, doi:10.1088/1748-9326/8/3/034014.

Johnson, R. S., J. Ayars, and T. Hsiao (2002), Modeling young peach tree evapotranspiration, *Acta Hortic.*, *584*, 107–113.

Johnson, R. S., J. Ayars, and T. Hsiao (2004), Improving a model for predicting peach tree evapotranspiration, *Acta Hortic.*, *664*, 341–346.

Johnson, R. S., L. E. Williams, J. E. Ayars, and T. J. Trout (2005), Weighing lysimeters aid study of water relations in tree and vine crops, *Calif. Agric.*, *59*(2), 133–136.

Kanamaru, H., and M. Kanamitsu (2008), Model diagnosis of nighttime minimum temperature warming during summer due to irrigation in the California Central Valley, *J. Hydrometeorol.*, *9*, 1061–1072.

Kueppers, L., and M. Snyder (2012), Influence of irrigated agriculture on diurnal surface energy and water fluxes, surface climate, and atmospheric circulation in California, *Clim. Dyn.*, doi:10.1007/s00382-011-1123-0.

Kueppers, L., M. Snyder, and L. Sloan (2007), Irrigation cooling effect: Regional climate forcing by land use change, *Geophys. Res. Lett.*, *34*, L03703, doi:10.1029/2006GL028679.

Kueppers, L., et al. (2008), Seasonal temperature response to land-use change in the western United States, *Global Planet. Change*, *60*, 250–264.

Leung, R., and Y. Qian (2009), Atmospheric rivers induced heavy precipitation and flooding in the western U.S. simulated by the WRF regional climate model, *Geophys. Res. Lett.*, *36*, L03820, doi:10.1029/2008GL036445.

Lo, M., and J. Famiglietti (2013), Impact in California's Central Valley strengthens the southwestern U.S. water cycle, *Geophys. Res. Lett.*, *40*, 301–306, doi:10.1002/grl.50108.

Lobell, D., and C. Bonfils (2008), The effect of irrigation on regional temperatures: A spatial and temporal analysis of trends in California, 1934–2002, *J. Clim.*, *21*, 2063–2071.

Lobell, D., G. Bala, A. Mrin, T. Phillips, R. Maxwell, and D. Rotman (2009), Regional differences in the influence of irrigation on climate, *J. Clim.*, *22*, 2248–2255.

Mahmood, R., et al. (2010), Impact of land use/land cover change on climate and future research priorities, *Bull. Am. Meteorol. Soc.*, doi:10.1175/2009BAMS2769.1.

Mu, Q., M. Zhao, and S. W. Running (2011), Improvements to a MODIS global terrestrial evapotranspiration algorithm, *Remote Sens. Environ.*, *115*, 1781–1800.

Owe, M., R. de Jeu, and T. Holmes (2008), Multisensor historical climatology of satellite-derived global land surface moisture, *J. Geophys. Res.*, *113*, F01002, doi:10.1029/2007JF000769.

Ozdogan, M., M. Rodell, H. Beaudoing, and D. Toll (2010), Simulating the effect of irrigation over the United States in a land surface model based on satellite-derived agricultural data, *J. Hydrometeorol.*, *11*, 171–184.

Pielke, R. A., Sr., et al. (2011), Land use/land cover changes and climate: Modeling analysis and observational evidence, *WIREs Clim. Change*, *2*, 828–850, doi:10.1002/wcc.144.

Pokhrel, Y., et al. (2012), Incorporating anthropogenic water regulation modules into a land surface model, *J. Hydrometeorol.*, *13*, 255–269.

Pu, B., and R. Dickinson (2012), Examining vegetation feedbacks on global warming in the Community Earth System Model, *J. Geophys. Res.*, *117*, D20110, doi:10.1029/2012JD017623.

Ramankutty, N., A. T. Evan, C. Monfreda, and J. A. Foley (2008), Farming the planet: 1. Geographic distribution of global agricultural lands in the year 2000, *Global Biogeochem. Cycles*, *22*, GB1003, doi:10.1029/2007GB002952.

Sacks, W., B. Cook, N. Buenning, S. Kevis, and J. Helkowski (2009), Effects of global irrigation on the near-surface climate, *Clim. Dyn.*, *33*, 159–175.

Schaake, J., V. Koren, Q. Duan, K. Mitchell, and F. Chen (1996), A simple water balance model (SWB) for estimating runoff at different spatial and temporal scales, *J. Geophys. Res.*, *101*, 7461–7475, doi:10.1029/95JD02892.

Segal, M., Z. Pan, R. Turner, and E. Takle (1998), On the potential impact of irrigated areas in North America on summer rainfall caused by large-scale system, *J. Appl. Meteorol.*, *37*, 325–331, doi:10.1175/1520-0450-37.3.325.

Sorooshian, S., J. Li, K. Hsu, and X. Gao (2011), How significant is the impact of irrigation on the local hydroclimate in California's Central Valley? Comparison of model results with ground and remote-sensing data, *J. Geophys. Res.*, *116*, D06102, doi:10.1029/2010JD01775.

Sorooshian, S., J. Li, K. Hsu, and X. Gao (2012), Influence of irrigation schemes used in RCMs on ET estimation: Results and comparative studies from California's Central Valley agricultural regions, *J. Geophys. Res.*, *117*, D06107, doi:10.1029/2011JD016978.

Tang, Q., S. Peterson, R. H. Cuenca, Y. Hagimoto, and D. P. Lettenmaier (2009), Satellite-based near-real-time estimation of irrigated crop water consumption, *J. Geophys. Res.*, *114*, D05114, doi:10.1029/2008JD010854.

Wei, H., Y. Xia, K. E. Mitchell, and M. B. Ek (2012), Improvement of Noah land surface model for the warm season processes: Assessment of water and energy flux simulation, *Hydrol. Processes*, doi:10.1002/hyp.9214.

Wei, J., P. A. Dirmeyer, D. Wisser, M. G. Bosilovich, and D. M. Mocko (2013), Where does the irrigation water go? An estimate of the contribution of irrigation to precipitation using MERRA, *J. Hydrometeorol.*, *14*, 275–289.

Wichelns, D., and D. Nelson (1989), An empirical model of the relationship between irrigation and the volume of water collected in subsurface drains, *Agric. Water Manage.*, *16*, 293–308.

Wisser, D., S. Frolking, E. Douglas, B. Fekete, C. Vorosmarty, and A. Schumann (2008), Global irrigation water demand variability and uncertainties arising from agriculture and climate data sets, *Geophys. Res. Lett.*, *35*, L24408, doi:10.1029/2008GL035296.

Xia, Y., et al. (2012a), Continental-scale water and energy flux analysis and validation for the North American Land Data Assimilation System project phase 2 (NLDAS-2): 1. Intercomparison and application of model products, *J. Geophys. Res.*, *117*, D03109, doi:10.1029/2011JD016048.

Xia, Y., et al. (2012b), Continental-scale water and energy flux analysis and validation for North American Land Data Assimilation System project phase 2 (NLDAS-2): 2. Validation of model-simulated streamflow, *J. Geophys. Res.*, *117*, D03110, doi:10.1029/2011JD016051.